Suresh Goyal
Wireless Research Laboratory
Lucent Technologies
Bell Laboratories
600 Mountain Avenue, Rm. 1B-212
Murray Hill, NJ 07974

Jim M. Papadopoulos
Rexnord Technical Services
5101 West Beloit Road
West Milwaukee, WI 53214

Paul A. Sullivan
Wireless Research Laboratory
Lucent Technologies
Bell Laboratories
600 Mountain Avenue, Rm. 1C-326
Murray Hill, NJ 07974

Shock Protection of Portable Electronic Products: Shock Response Spectrum, Damage Boundary Approach, and Beyond

The pervasive shock response spectrum (SRS) and damage boundary methods for evaluating product fragility and designing external cushioning for shock protection are described in detail with references to the best available literature. Underlying assumptions are carefully reviewed and the central message of the SRS is highlighted, particularly as it relates to standardized drop testing. Shortcomings of these methods are discussed, and the results are extended to apply to more general systems. Finally some general packaging and shock-mounting strategies are discussed in the context of protecting a fragile disk drive in a notebook computer, although the conclusions apply to other products as well. For example, exterior only cushioning (with low restitution to reduce subsequent impacts) will provide a slenderer form factor than the next best strategy: interior cushioning with a "dead" hard outer shell. © 1997 John Wiley & Sons, Inc.

INTRODUCTION AND SCOPE

When two bodies contact with a finite (nonzero) approach velocity, the resulting collision is termed *impact*. The absorption or storage of kinetic energy, within a small relative displacement (or interpenetration), gives rise to extremely high contact forces. Components are usually joined without any free play in order to prevent impact.

The modeling of impact to determine the contact force and the potential for yield or fracture will not be taken up here. Suffice it to say that compact, solid bodies tend to have their highest stresses near the contact region and tend to suffer local denting or crushing. Nonsolid systems may have even higher stresses at narrow ligaments or connectors. Structures formed of slender transverse members (plates or beams) tend to be the most compliant, deforming globally by bending or torsion, even to the point of failure.

Our present interest in impact damage concerns the failure of components *suspended internally* to

the main structure. Common examples include the display or disk drive of a portable computer, a ceramic substrate in a cellular telephone, the filament of a projection lamp, or a product in its shipping container. The dynamics of small internal suspended parts during an impact is known as *shock response*.

Market research has shown that *mobility enhancing products* like cellular telephones, laptop computers, etc., are more likely to gain wide customer acceptance if they are rugged; i.e., they can withstand accidental drops from modest heights and occasional bangs against hard surfaces. However, requirements for this "impact tolerance" are stringent. To name a few, it must protect fragile elements like liquid crystal displays (LCDs), disk drives, ceramic modules, brittle interconnects, etc., from several impacts over the product's lifetime. It must be extremely compact and not make the product look bulky or unappealing. The product should not suffer even cosmetic damage when dropped.

For perspective, note that an end user may drop or bang the product more than the shipper, but without the large stopping distances and penetration resistance afforded by thick foam cushions and sturdy shipping cartons. In a portable consumer product, cushioning bulk must be measured in millimeters, not inches!

Consider a notebook computer containing a fragile component like a hard disk drive, which is known to be damaged by acceleration exceeding $500 \times g$. (Components whose fragility derives from internal suspended elements may withstand brief pulses of much higher acceleration, thanks to internal stopping distance. This additional protection is covered in a later section on *critical velocity*). If the computer is dropped from shoulder height (roughly 60 in.), we may compute a lower bound on the safe stopping distance as

$$\frac{1 \times g}{500 \times g} \, 60 \text{ in.} = 0.12 \text{ in.}$$

This is the very smallest possible stopping distance for the fragile component, assuming a uniform, maximal braking force and no damaging internal vibrations.

However, in practice that stopping distance should probably be multiplied by a factor to account for the nonconstant "spring" force arising from deformation of the interior suspension and exterior housing (factor $= \sqrt{2}$ when suspension or cushioning are modeled as a linear spring). If

the outer cushioning interacts poorly with the inner suspension, the total distance may have to be multiplied by another factor of 2 or even more.

Thus, the composite stopping distance to prevent damage can easily exceed 0.3 in. and there can be even less desirable configurations requiring further stopping distance. Providing this stopping distance in every direction would make the product a lot bulkier. It is important, therefore, to use shock-resistant components and to employ padding efficiently.

This article focuses on issues of shock modeling, testing, and protection. Conceptually, the subject divides naturally into two parts: impact-induced motion of the "suspension point" that supports the fragile element and the consequent dynamic response of the element. For each of these parts, the approach is to classify typical properties and behaviors; the resulting potential for damage is then either intuitively obvious or can be assessed easily.

Of course, the most important part of the subject consists of strategies and guidelines for modifying the system to prevent damage, within space and mass constraints. This may be done with external cushioning, interior suspension, alteration of suspended natural frequency, or with a more shock-resistant part.

The scientific literature on shock remains relatively inaccessible to designers. Part of our aim in this work is to introduce and critique it, and where possible to extend it. Unlike prior work that often focused on protective packages for shipping (where dimensions are virtually unrestricted), we seek to reduce both cushion thickness and "sway space" (allowable deformation or displacement of various components), because these are so restricted in compact electronic products.

SHOCK ANALYSIS ASSUMPTIONS AND APPROACHES

When a body or system undergoes impact, the geometry, materials, and connections dictate the motions of its constituent parts. Typically, every part of the body undergoes a significant change of velocity during a few milliseconds, and large periodic accelerations may continue due to residual vibration or "ringing."

Our focus is on some subsidiary fragile part of the system, such as a disk drive, LCD, etc. To fall within the scope of usual shock analysis methods, it must satisfy the following criteria:
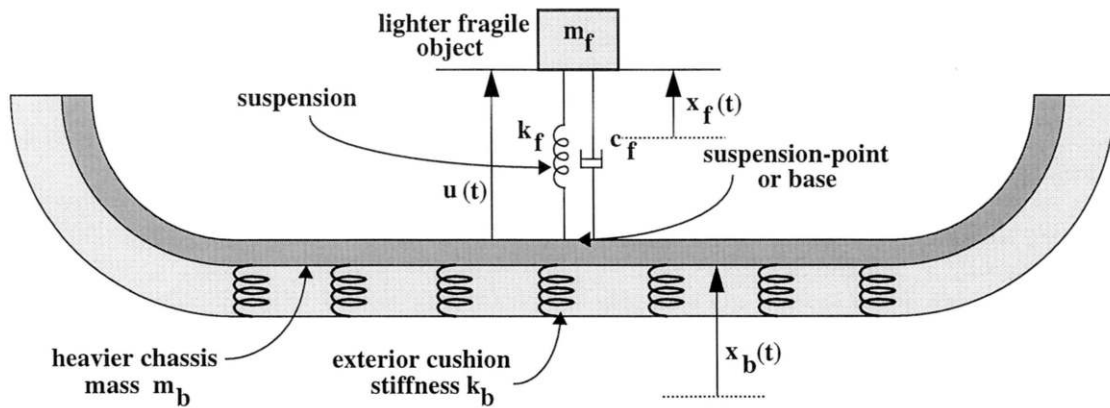
FIGURE 1 Schematic of a portable product for shock analysis.

1. The fragile part must be considerably smaller in mass than the system (or part thereof) to which it is joined. Then coupling can be considered one way, i.e., fragile part vibrations can be reasonably supposed to not affect the system's motion.
2. The fragile part must not be a load-bearing structural element; it has to be "suspended" without prestress within the main system. Then the only significant forces it experiences are proportional to its acceleration.
3. In combination with its suspension elements, the fragile subpart must be well approximated by a mass-spring or mass-spring–damper model. (If the first assumption really holds, then a tap on the fragile part will reveal its dynamic characteristics.)
4. It should not display any internal dynamics (i.e., to first order, the fragile part can be modeled as a rigid mass). Then the peak acceleration that it undergoes, *solely* determines whether damage occurs. (Exceptions to this requirement will be considered below.)

If the above four conditions are met, as typified in the system shown schematically in Fig. 1, the following approach is sensible for understanding shock response:

1. Measure or otherwise characterize the impact-induced motion of the fragile element's suspension point (the mounting point or the base of the suspension). This will be taken as the forcing displacement $x_b(t)$ applied to the "base" of the suspended fragile element, henceforth referred to only as the suspension point.

2. Recall that the equation of motion for a viscoelastically suspended fragile mass, forced by the motion of its suspension point, can be written either in terms of its absolute motion $x_f(t)$, or in terms of its relative motion $u(t) = x_f(t) - x_b(t) \Rightarrow m\ddot{x}_f = -g(u, \dot{u})$, where g is a response function giving the suspension force, acting on the mass in the positive u direction, in terms of the mass' relative displacement and velocity.
3. Assume that limiting (damaging) conditions are defined either by the fragile object's peak acceleration exceeding some critical acceleration, a_{cr}, i.e., $\ddot{x}_f^{max} = \ddot{u} + \ddot{x}_b > a_{cr}$, or by its peak relative displacement exceeding some critical displacement, u_{cr}, i.e., $u^{max} > u_{cr}$. Note that these peak values do not occur simultaneously unless the suspension is purely elastic. The peaks may occur at any times during or after the impact; the need to determine these intervals is a complicating feature of any analytical investigation.

For impact tolerance, damage thresholds are usually not specified in terms of allowable stresses and strains because at the component and product level, peak accelerations and displacements are the most measurable and useful/meaningful parameters; this will also become clearer through this article. However, determining these acceleration/displacement thresholds is a nontrivial task, either because component manufacturers cannot provide them (the migration of desktop technologies to portable devices being fairly new, component manufacturers, at best, provide rudimentary damage thresholds that are usually unreliable) or they are just complicated.

Consider for instance the problem of determin-

ing a_{cr} for a disk drive. If positional inaccuracies of the read/write head over the platter constitutes drive failure and the cantilevered suspension of the head is purely elastic, a_{cr} would be the acceleration corresponding to the maximum tolerable locational inaccuracy. However, if the damage mechanism was the head striking against the rigid platter, the problem becomes nonlinear and it would be difficult to measure a_{cr} because the drive would be able to sustain a much higher level of quasistatically imposed acceleration than a dynamic one. It is as if we would have to define two kinds of critical accelerations.

SHOCK ANALYSIS

The general shock problem arises from the impact of a moving (falling) object with a floor, desk, or wall, generally something more massive by far. The "magnitude" of the collision is defined by the velocity of impact (or the drop height). The concern is that some interior part of the device will suffer such a high stress in the collision that it is damaged. Or, perhaps some internal deflection limit will be exceeded, disrupting proper functioning. The first step in shock analysis is to recognize that the suspension point of a fragile component undergoes a sudden variation in velocity due to the collision. [Note that it is suspension point *acceleration* that forces the relative-motion equation, $m\ddot{u} + c\dot{u} + ku = -m\ddot{x}_b(t)$.]

In what follows, it is important to distinguish between *suspension* and *cushioning*. As we use these terms here, suspension is internal, i.e., the grommets or structural compliance connecting the fragile element to its suspension point. In contrast, cushioning is external, i.e., rubber feet or housing overmold interposed between the chassis and ground.

Shock Induced Suspension Point Motion

The exact nature of the suspension point motion may be very hard to predict, but just a few characteristics are important. First, there is a net change of mean velocity Δv due to the impact. The system may have a substantial rebound elastically, in which case the mean suspension point velocity suffers a change $\Delta v = 2v_0$, where v_0 was the downward velocity of the suspension point just before the collision. Or it may come completely to rest, in which case $\Delta v = v_0$. In an intermediate case,

$$\Delta v = (1 + e)v_0 = \int_0^\tau \ddot{x}_b(t)\, dt, \qquad (1)$$

where e is the coefficient of restitution. In either case, Δv is just the area under the acceleration-time record for $x_b(t)$.

The essence of this record, frequently a unimodal pulse, is typically described rather simply. For the given velocity change, i.e., area, the acceleration pulse will either be narrow and high or wide and low. Roughly speaking, it can be characterized by its magnitude and duration. A particularly useful measure of pulse duration is its *effective duration*, τ_{eff}, defined as

$$\tau_{eff} \equiv \frac{\text{pulse area}}{\text{pulse magnitude}} = \frac{\int_0^\tau a_b(t)\, dt}{a_b^{max}}, \qquad (2)$$

where $a_b(t)$ is the acceleration shock pulse applied to the base. (Note that if the chassis and cushioning can be modeled as a linear spring, then pulse duration is affected only by their stiffness and not the impact velocity v_0.)

A more complete pulse specification must include the pulse shape, but it is considered that a broad range of shapes is more or less similar. The key information relates to spectral content: does the pulse rise and fall relatively gently? Or do level changes occur extremely rapidly (and thus contain significant high-frequency components)?

Finally, it may occur (either for a "free" rebounding system, or for a "dead" nonrebounding supported one) that after the change in mean velocity Δv there remains a residual oscillation or ringing at a natural frequency of the unsupported system.

The acceleration pulse experienced near the impact point (the outermost point that makes contact with the other colliding surface) is extremely high and very short, because it comes to rest almost instantaneously. Even if the system mass center is in the process of rebounding elastically, there is a comparatively long period during which contact-point acceleration is zero while the rest of the system first compresses and then recovers (the "restitution phase" of the collision). The contact point will experience a second sharp acceleration spike if it leaves the floor.

The acceleration pulse at more distant points on the deformable body consists of smaller and more rounded leading and trailing spikes, which are typically blended with a compensatingly higher pulse between them. At points that are sufficiently
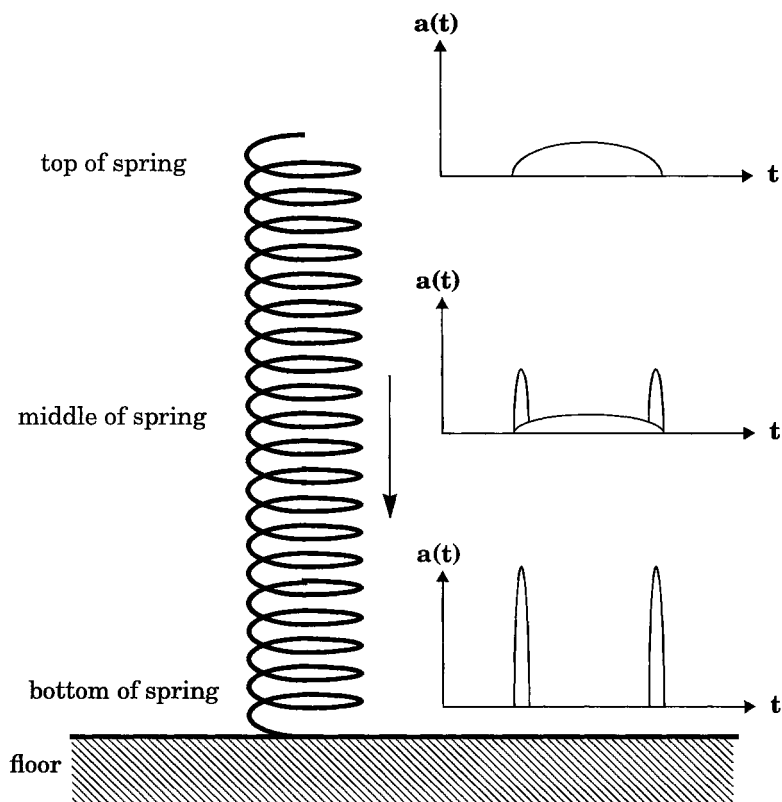
FIGURE 2 Rough sketch of the acceleration pulses that may be experienced at various points of a linear spring as it collides vertically with a hard floor.

far removed or are shielded by strain-wave reflecting impedance changes (like concentrated masses), the pulse may be smooth and essentially unimodal.

A simple way to visualize the pattern of acceleration pulses is to consider the various points of a mass-bearing spring striking and rebounding from a hard floor. This scenario is roughly sketched in Fig. 2.

Depending on the modes and damping of the system, postimpact vibration at the suspension point may be substantial. For example, if two equal masses are joined by a soft elastic spring and the bottom mass rebounds quickly from a stiff elastic floor, then virtually all the initial kinetic energy will have been converted to vibrational energy. This is because the center of mass (CM) of the two-mass system has initial momentum $-2m * v_0$ that is changed by $2 * (m * 2v_0)$ due to two elastic collisions of the bottom mass with the floor. The two masses then oscillate about the CM (which is moving up with velocity v_0) with equal and opposite velocities.

To summarize, the shock induced motion of the

base of the suspension point may be a smooth unimodal acceleration pulse, a pulse with leading (and possibly trailing) spikes, or a more complex waveform with several oscillations and spikes. When it is too difficult to calculate this pulse, measuring it is the only alternative. To make this measurement, a high-bandwidth accelerometer must be rigidly attached to the suspension point, perhaps in place of the suspended fragile element.

Suspended Component Response to Suspension Point Accelerations

Given the "forcing acceleration pulse" produced at the suspension point from the impact of the chassis with the ground, how does the suspended system respond to this input and when does damage occur?

However a fragile part is supported, the *net force* exerted on it equals its mass times its acceleration. When the net force is great enough, it will damage either the part or its support. In the shock problem, it is reasonable to say that the forcing *input* is a suspension point acceleration pulse,

while the *outputs* or consequences of concern are the fragile-body acceleration and peak relative displacement (where it may impact a structural member). The most common shock response calculations are those evaluating peak fragile-element acceleration due to a range of acceleration pulse inputs.

With a good model for the suspended system, it would be possible to calculate the peak acceleration caused by suspension point acceleration. One way to develop that model is to tap the suspended fragile element and determine its mass, undamped natural frequency, and damping ratio. (Remember, it is assumed that suspended object dynamics are not coupled to those of the larger system.) Referring to Fig. 1, frequently used model parameters for the lighter fragile component and its suspension are the undamped natural frequency, $\omega_n = \sqrt{k_f/m_f}$, and the time period of free oscillation $T_n = 2\pi/\omega_n$; and for the heavier chassis the parameter is the natural frequency Ω_n.

Because input and output accelerations are central to shock response, it bears noting that variable upwards suspension point acceleration is rigorously equivalent to a fixed suspension point and variable downward gravity in its effects on suspension displacements (i.e., relative motions) and fragile-element forces. Frequently the second case is easier to envision. (This analogy holds true for systems of any complexity.)

SHOCK RESPONSE FOR SHORT AND LONG PULSES: LIMITING BEHAVIORS

It is possible to describe the shock response for pulses of short and long durations (short pulses and long pulses, respectively) without performing detailed analyses. In brief, the effects of a short pulse depend only on the velocity it imparts (i.e., the Δv causing it); long pulses accelerate the fragile element just the same as the base, unless they have fast rise times.

Acceleration Pulse Considerably Shorter than T_n

If the duration of the shock pulse experienced by the base is considerably shorter than the time period of free vibration of the fragile system, T_n, the peak fragile-element acceleration will depend *only* on the velocity change of the base and *not* on the time period over which it occurs.

That this must be so for arbitrary acceleration

pulse shapes *and even for multiple degree of freedom (MDOF) nonlinear systems* can be seen by either of the following two arguments. First, if the base is accelerated to its final (upward) velocity so quickly that it barely moves during the process, the dynamics problem is equivalent to one in which the base is at rest and all masses start with identical downward initial velocities. (The MDOF can arise from the product having multiple fragile parts or one or more suspended masses *between* the outer casing and the fragile system.)

Alternatively, it may be recalled that a varying base acceleration is dynamically exactly equivalent to a varying body force (like gravity force) applied to all masses in the system, while the base is held fixed. If the time period of force application is sufficiently short compared to the shortest system response time (i.e., vibration period), the bodies do not alter their positions much, and simply undergo accelerations directly proportional to the impressed "gravity." The result is that at the end of an arbitrary brief pulse of base acceleration, all masses are in essentially their initial positions, with identical velocities relative to the base.

However this argument is rationalized, it is clear that the subsequent peak internal acceleration in the system depends only on the magnitude of the velocity imparted to the base.

These ideas give rise to the very important notion of "velocity shock": a base acceleration for a sufficiently short time period whose effects depend only on the net velocity imparted, not on the pulse's shape, peak magnitude, or precise duration. The notion of velocity shock is applicable generally to all well-behaved systems. A velocity shock just great enough to cause damage defines a "critical velocity," v_{cr} (to be discussed in a later section).

There are two ways a velocity shock might harm a fragile component. One is when the initial (relative) velocity causes motion whose peak acceleration equals a_{cr}. This is the normal velocity shock limit and may be calculaated as $v_{cr} = a_{cr}/\omega_n$. The other way a velocity shock might cause damage is where the sway space is too small, and the fragile element "slaps" into a nearby structure, in a motion whose acceleration otherwise would not be critical. This interior impact or slap causing critical velocity may be calculated as $v_{cr}^{slap} = u_{cr}\omega_n$, where u_{cr} is the relative interior displacement (or sway) that leads to impact. However, v_{cr}^{slap} implies that a_{cr} is reached only with the suspension at the interior sway limit, which invalidates the dynamic model. So we will discuss the interior sway limit primarily

for the purpose of ensuring that it is never encountered; i.e., ω_n should be adjusted so that $\omega_n^2 \geq a_{cr}/u_{cr}$.

For the damped single DOF (SDOF) fragile system depicted in Fig. 1, the relationship between a_{cr} and v_{cr} can be found by subjecting its base to a short-pulse shock of area v_{cr}. This is equivalent to applying a step change in velocity to the base of magnitude v_{cr}. From the Appendix we find that the peak acceleration of the fragile system a_{cr} would then be

$$a_{cr} = \begin{cases} -\dfrac{\zeta}{\sqrt{1-\zeta^2}} \tan^{-1}\left(\dfrac{\sqrt{1-\zeta^2}(4\zeta^2-1)}{\zeta(4\zeta^2-3)}\right) \\ -v_{cr}\omega_n e & \text{for } 0 \leq \zeta \leq 0.5, \\ -2v_{cr}\omega_n\zeta & \text{for } 0.5 < \zeta \leq 1, \end{cases} \tag{3}$$

where damping ratio $\zeta = c_f/2\sqrt{k_f m_f}$. It can be seen that for a purely elastic suspension, as mentioned earlier, the relationship is very simple: $v_{cr} = a_{cr}/\omega_n$. (This should be obvious: in a freely vibrating mass-spring system, peak acceleration is related to peak velocity by the factor ω_n).

MDOF, and even nonlinear systems, each have their own relation defining acceleration-limited v_{cr} in terms of a_{cr} and system parameters; but these are not so simply found!

Acceleration Pulse Considerably Longer than T_n

If the duration of the shock pulse experienced by the base is considerably longer than T_n, there are two cases to consider. The first is if the pulse is gently increasing and gently decreasing (like a very wide half-sine), there will be no suspended object transients. The fragile system will respond quasi-statically to the imposed acceleration level ($a_f^{max} = a_b^{max}$) and damage will occur only if the imposed acceleration magnitude exceeds a_{cr}. (Because system response time is much shorter than the forcing pulse rise time, fragile-system acceleration will closely track the applied pulse, thereby appearing as if the shock pulse was applied quasi-statically.) This is a perfectly general result that requires no further qualification. The second case is if the pulse has a rapid rise time, no matter how broad it is, its frequency content will excite overshoot. For example, for the damped SDOF system of Fig. 1, if a step acceleration of magnitude a_b^{max} were to be applied to its base, fragile-system peak response, as shown in the Appendix, would be

$$a_f^{max} = a_b^{max}$$

$$+ \begin{cases} a_b^{max} e - \dfrac{\zeta}{\sqrt{1-\zeta^2}}\left(\tan^{-1}\left(\dfrac{2\zeta\sqrt{1-\zeta^2}}{2\zeta^2-1}\right)+\pi\right) \\ \qquad\qquad\qquad \text{for } 0 \leq \zeta \leq \sqrt{0.5}, \\ a_b^{max} e - \dfrac{\zeta}{\sqrt{1-\zeta^2}} \tan^{-1}\left(\dfrac{2\zeta\sqrt{1-\zeta^2}}{2\zeta^2-1}\right) \\ \qquad\qquad\qquad \text{for } \sqrt{0.5} < \zeta \leq 1. \end{cases} \tag{4}$$

It can be seen from Eq. (4) that for a purely elastic suspension $a_f^{max}/a_b^{max} = 2$, i.e., the transient response is twice the longer term static response. (This is a well-known result for suddenly applied loads.) So damage will occur if a fast-rising acceleration pulse's magnitude exceeds $a_{cr}/2$. When damping is significant the ratio of transient response to longer term static response, a_f^{max}/a_b^{max}, is somewhere between 1 and 2. Note that the higher the damping, the lower the ratio is.

Although similar fast-rise/long-duration shock behavior will also occur for undamped or damped MDOF systems (and even for some nonlinear ones), the resulting peak fragile-component acceleration can be far more than twice as great. As an example, one may have a lightly damped MDOF system where the shock pulse from the point of impact is transformed into a sustained oscillation at the fragile-component suspension point, forcing it into resonance (e.g., Mindlin, 1945, fig. 3.5.2, p. 432).

REPRESENTING SHOCK RESPONSE

The acceleration of a suspended fragile element, in response to the base excitation of its suspension point, is represented in two different ways. One is as a ratio between the peak imposed base acceleration and the peak element response acceleration, which is plotted as a function of excitation pulse duration and is called the shock response spectrum (SRS). The other approach is to define the set of pulses that just cause damage, based on their amplitude and area (i.e., Δv), via the damage boundary plot.

SRS Approach

To characterize suspended system shock susceptibility, unimodal acceleration pulses of various

fixed shapes (like rectangular, trapezoidal, sinusoidal, versed sine, triangular, sawtooth, etc.) are applied to the system's suspension point, and the peak acceleration suffered during or after the pulse by the fragile part is determined. [Oscillatory base pulses are rarely applied in the SRS literature. The topic is usually treated via a higher order system model, with a large mass between the accelerated base and the suspended fragile element (e.g., Mindlin, 1945, p. 431). This brings in modeling issues and provides less general plotted conclusions.]

Assuming that the system's dynamic response, when subjected to the above pulses, can be approximated with that of a linear dynamic system, the so-called "base pulse response ratio $\mathbf{R}$" is evaluated as a function of pulse duration.

$$\mathbf{R} = \frac{\text{fragile-part response acceleration peak magnitude}}{\text{suspension-point acceleration pulse peak magnitude}}$$

$$= \frac{a_f^{max}}{a_b^{max}} = \frac{|\ddot{u} + a_b|^{max}}{a_b^{max}} \, . \tag{5}$$

To state it more mathematically, a_f^{max} is the maximum of $|\ddot{u} + a_b|$ over $0 \leq t \leq \infty$, where u is calculated from the SDOF equation of motion,

$$m\ddot{u} + g(u, \dot{u}) = -ma_b(t), \tag{6}$$

where $a_b(t)$ is the acceleration pulse applied to the base. Note that the *peak* fragile-part acceleration does not occur at any fixed interval after the collision begins; t_{peak} must be determined.

System response could equivalently be defined in terms of the peak value of fragile-element force, $m\ddot{x}_f^{max}$, divided by the force it would experience if forcing-pulse period and rise times were long: $m\ddot{x}_b^{max}$. For purely elastic (undamped) suspensions, the peak acceleration is equivalent to the peak sway: $m\ddot{x}_f^{max} = Ku^{max}$. In this case some authors define the peak force for quasistatic response in terms of an artificial displacement: $m\ddot{x}_b^{max} = ku_{quasistatic}^{max}$. The acceleration response ratio can then be replaced by an equivalent displacement ratio $u^{max}/u_{quasistatic}^{max}$.

The plot of base pulse response ratio versus pulse duration, called the SRS, or *maximax response spectrum*, is discussed in detail in Ayre (1988), Mindlin (1945), Newton (1968, 1988, 1989), and Rubin (1988). It is used quantitatively by establishing the effective duration and magnitude of the acceleration pulse arising from the impact of

a cushioned chassis hitting the ground with velocity v_0. The resulting peak acceleration of the suspended fragile element can be determined from $\mathbf{R}$. If it is less than a_{cr}, the fragile object will not be damaged. However, in measuring the acceleration of just one putative fragile element, the SRS says nothing about the potential for damage elsewhere.

A slightly different treatment, considering full-spectrum excitation of many internal DOF is outlined in Henderson (1993). In this method the SRS plot is presented as a spectral plot of the peak acceleration response ratios of an *infinite number of decoupled similar SDOF dynamic systems, covering the entire spectrum of time constants*. (Note that for excitation pulses of a fixed shape, both interpretations yield similar SRS plots.) However, in a portable product it is usually difficult to figure out those elements that are decoupled and fall within the precincts of the above SRS model. Additionally, it is not clear if this method yields any insights or inferences that cannot be drawn from the original interpretation.

A sample SRS plot for an SDOF system is plotted in Figs. 3 and 4. Note that the response ratio $\mathbf{R}$ (ordinate) is plotted against the ratio of the effective duration of the basal shock pulse [as defined in Eq. (2)] to the time period of free vibration of the fragile system, τ_{eff}/T_n (abscissa). The family of unimodal pulse shapes employed in these plots includes a half-sine [as might be expected in an elastic collision where the compliance is concentrated at the contact (padding), or where a single mode only is excited] as well as symmetric-triangular and versed sine pulse shapes meant to encompass various cushioning-material behaviors. Because pulses with fast rise and decay times will potentially excite the greatest internal transients, a rectangular pulse shape is chosen as a worst case and as can be seen from the plot for a given pulse amplitude and duration, a rectangular pulse shape does indeed generate the highest response ratio. [In practice, a more practical realization of a rectangular pulse, viz., a trapezoidal pulse with very fast rise and decay times, it used to simulate worst likely excitation. Asymmetric-triangular pulses (which also have high spectral content) have been explored by Mindlin (1945, fig. 3.8.2, p.445) and Ayre (1988). In general, their responses are not too different from their symmetric counterparts if they rise and decay fairly slowly; fast-falling asymmetric pulses lead to lower responses than fast-rising ones.]
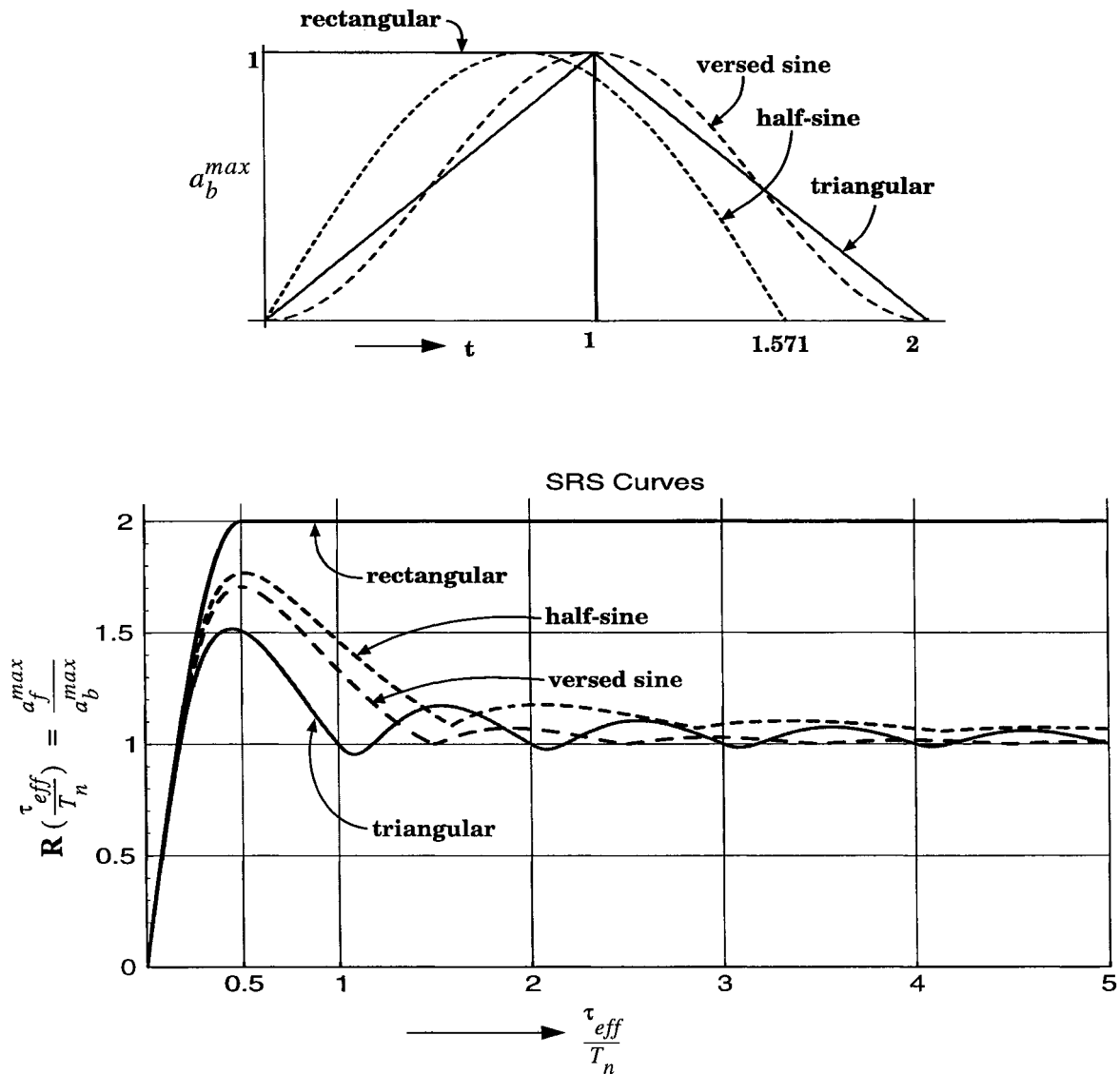
The expression representing the shock pulses

FIGURE 3 Shock response spectrum (SRS) plot for an undamped suspended mass.

used in our SRS plot, in terms of their *actual durations* τ, and the corresponding acceleration responses of the fragile mass are tabulated in the Appendix. The effective durations for the pulses can be calculated from τ as

$$\tau_{\text{eff}} = \begin{cases} \tau & \text{for rectangular pulses,} \\ \dfrac{2}{\pi}\tau & \text{for half-sine pulses,} \\ \dfrac{1}{2}\tau & \text{for versed-sine pulses,} \\ \dfrac{1}{2}\tau & \text{for symmetric-triangular pulses.} \end{cases} \tag{7}$$

Returning to the SRS plot of Fig. 4, observe that for $\tau_{\text{eff}}/T_n < 1/6$, *irrespective of pulse shape*, the SRS is approximately a straight line through the origin. This means that a base acceleration pulse of just half the duration, but of identical shape and magnitude, gives rise to just half the peak fragile-system acceleration. In other words, halving duration but doubling amplitude, *that is applying the same* Δv, leaves the internal peak accelerations (and hence potential for damage) unchanged. This is the short-pulse response discussed earlier. It is clear from Eq. (1) that for short-pulse shocks, it is advantageous to reduce e and hence Δv.

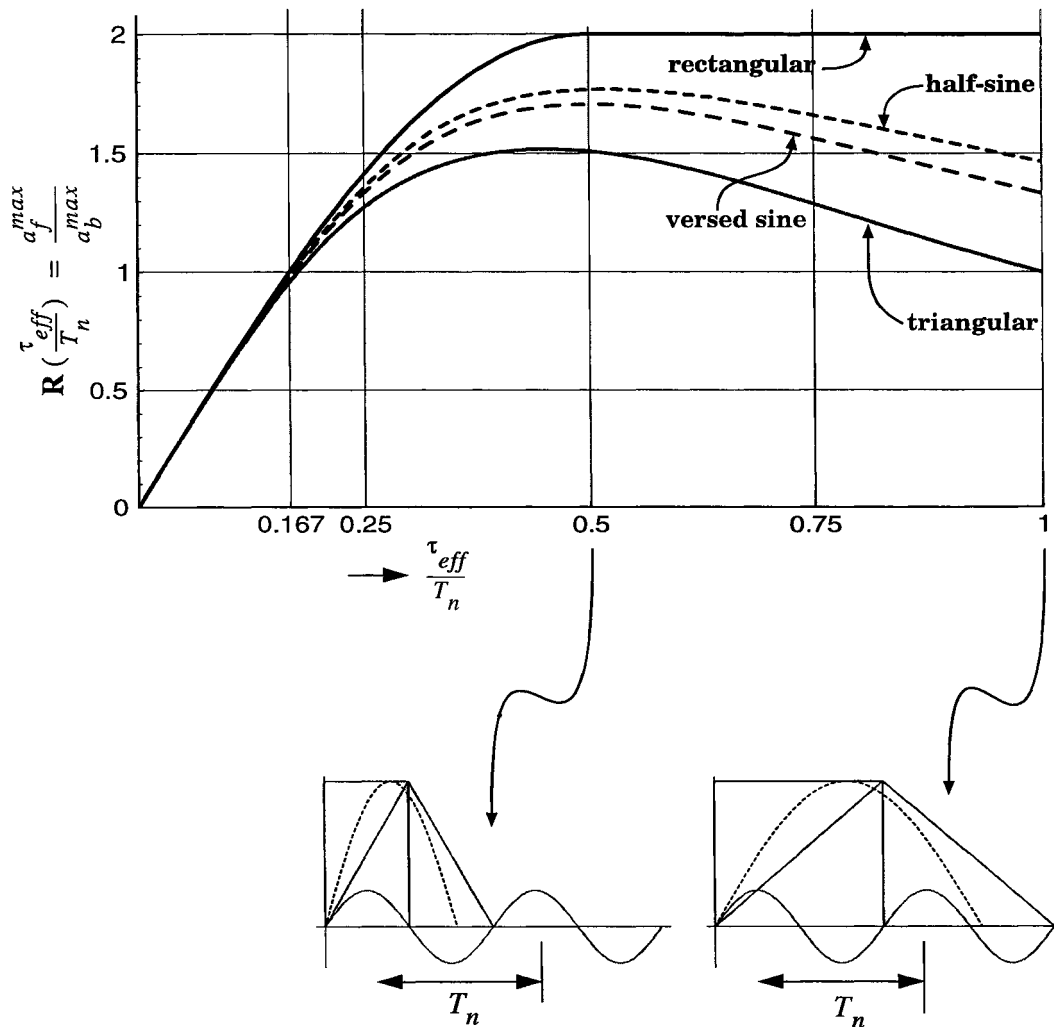At long pulse lengths the SRS becomes a horizontal line, of a level depending only on rise time.

Figure axis label: $R\left(\dfrac{\tau_{eff}}{T_n}\right) = \dfrac{a_f^{max}}{a_b^{max}}$

Curves labeled: **rectangular**, **half-sine**, **versed sine**, **triangular**

Horizontal axis: $\dfrac{\tau_{eff}}{T_n}$ with marks at 0.167, 0.25, 0.5, 0.75, 1

Insets labeled T_n and T_n

FIGURE 4   SRS plot of Fig. 3 drawn to higher resolution on the x axis. Insets show pulse durations in comparison to system free vibration time period for $\tau_{eff}/T_n = 0.5$ and 1.

This long-time response clarifies the value of cushioning, which transforms a given velocity change into an acceleration pulse of longer duration and lower magnitude.

The SRS plot allows the maximum permissible Δv to be read off for each duration of base acceleration pulse. Recall that for a linear cushion model, pulse length depends only on cushion properties. [Note that to determine the drop velocity from Δv requires a knowledge of restitution coefficient e. For first-order spring-damper cushion models, this is plotted in Goyal et al. (1994b, 1996).] By definition of τ_{eff}, the peak base acceleration arising from Δv is $\Delta v / \tau_{eff}$. The peak fragile-element acceleration is just this peak base acceleration, times $R(\tau_{eff}/T_n)$. We determine allowable Δv^{max} for each given τ_{eff}

by equating this peak fragile-element acceleration with a_{cr}. The result is

$$\Delta v^{max} = a_{cr}T_n \frac{\left(\dfrac{\tau_{eff}}{T_n}\right)}{R\left(\dfrac{\tau_{eff}}{T_n}\right)}. \tag{8}$$

The ratio of R to its argument is just the slope of a secant from the origin to the SRS point being considered. This slope is effectively constant for the initial straight-line section of the SRS, with the value $a_{cr}T_n/v_{cr}$. The slope decreases, implying that Δv^{max} increases, for all other points of the SRS, as may be seen by inspection.
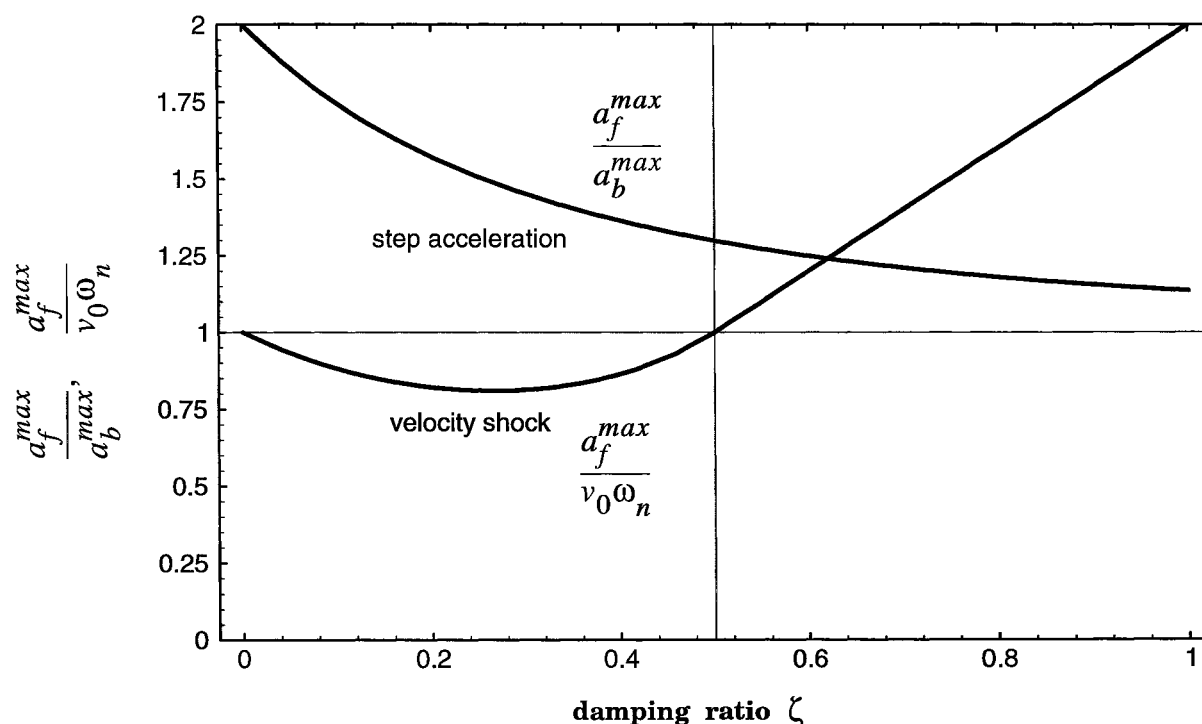
FIGURE 5 Effect of damping on the peak acceleration experienced by a suspended mass when subjected to (a) velocity shock, and (b) acceleration step function.

For a given base pulse shape and amplitude, the addition of damping to the suspension tends to reduce fragile-component peak acceleration, although the reduction follows different patterns for short and long pulses. Equation A.4 gives the maximum acceleration, as a function of damping ratio, for a linear spring-mass damper system subjected to a velocity shock of magnitude v_0. When plotted as a normalized curve of $a_f^{max}/v_0\omega_n$ versus ζ in Fig. 5, it clearly shows that $a_f^{max}/v_0\omega_n$ initially decreases from its undamped value with increasing damping ratio, reaches a minimum of 0.81013 for $\zeta = 0.2635$, and then begins to increase again with damping until $\zeta = 0.5$, beyond which additional damping becomes worse than having no damping at all! The upshot is that for velocity shocks moderate damping in the suspension, i.e., $\zeta < 0.5$, is beneficial.

However, when it comes to reducing the transient response from fast-rise long-duration pulses, the more the damping, the better it is! The plot of a_f^{max}/a_b^{max} [derived from Eq. (4), shown in Fig. 5] shows that in response to a step change in acceleration of the base, a_f^{max}/a_b^{max} decreases monotonically from its undamped value of 2 with increasing damping to the asymptotic value of the quasistatic response 1. (At very high values of ζ, the fragile

mass will be almost rigidly coupled to the base, thereby responding quasistatically to the imposed acceleration.)

Damage Boundary

In its simplest form, the damage boundary plot for the SDOF system considered in Fig. 3 is nothing but a replotting of its SRS plot in the $\Delta v - a_b^{max}$ plane, with appropriate transformations and scaling (Newton, 1968), to emphasize the importance of a v_{cr} and an a_{cr} for the system. A damage boundary plot for rectangular, half-sine, symmetric-triangular, and versed sine shock pulse shapes is plotted in Fig. 6. For simplicity, a_{cr} and T_n were set arbitrarily to equal unity, implying that $v_{cr} = 1/2\pi$. Appropriate values for the curves were obtained from the equations in the Appendix. The damage boundary plot is easier to apply than the SRS because Δv is used directly and there is no need to work with pulse duration.

When applied to a product with multiple fragile subsystems, perhaps even nonlinear, the damage boundary concept is actually more general than the SRS. The SRS merely presents acceleration amplification ratio for a single suspended subsystem, while the damage boundary presents the ac-
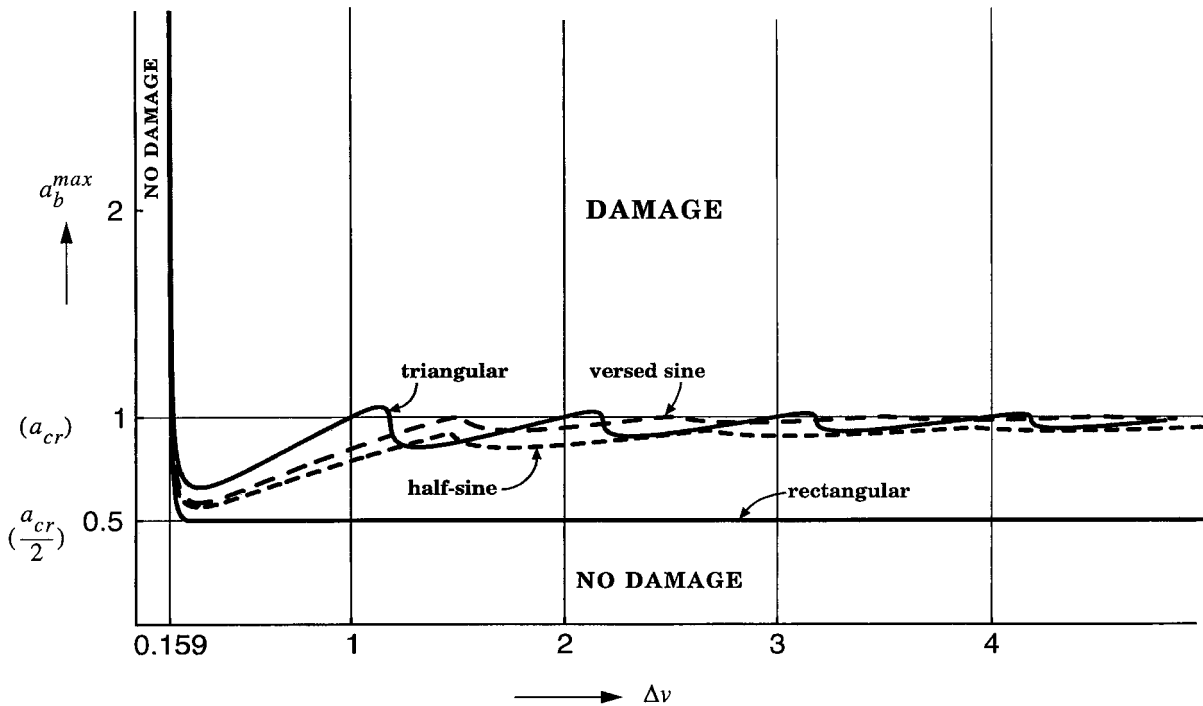
FIGURE 6 Damage boundary plot corresponding to the SRS shown in Fig. 3 for an undamped suspended mass.

tual shock parameters causing damage (whether one subsystem exceeded its a_{cr} or another exceeded its u_{cr}, etc.) for the entire product. The damage boundary plot can be interpreted as follows.

Every shock-acceleration pulse that the system is subjected to (implicitly, of fixed shape, e.g., sinusoidal or rectangular) can be plotted as a (pulse area, pulse magnitude) point on this graph and a boundary can be determined inside of which any pulse causes damage. The notion of critical velocity, i.e., of an impulsive housing velocity change, which does not quite cause damage no matter how great the peak acceleration, is represented by a vertical asymptote of abscissa v_{cr}. *Points to the left of this line represent shocks that cause no damage.* That is, any acceleration level is permitted as long as $\Delta v < v_{cr}$.

Points to the right of the v_{cr} asymptote refer to shocks that may cause damage unless sufficient cushioning is provided to reduce peak acceleration. In other words, as you move downward on the plot to lower peak accelerations for a given Δv, ultimately a point will be reached below which damage will no longer occur. The set of all such points constitutes a curve that completes the *damage boundary*. Shock pulses that lie below this curve will cause no damage; any Δv is permitted

as long as its $a < a_{cr}$. The lower arm of the damage boundary, corresponding to long-duration shock, is roughly parallel to the Δv axis. At very great collision velocities, a low-acceleration pulse must be extremely long and the damage boundary asymptotically approaches the a_{cr} ordinate, or some fraction thereof. For instance, if rectangular or fast-rising trapezoidal shock pulses are applied, in a linear system the transients will always multiply the internal accelerations and displacements beyond their quasistatic levels. So instead of a_{cr}, the horizontal boundary will approach ordinate a_{cr}/N. For an SDOF undamped system $N = 2$, and instead of gently rising asymptotic behavior the horizontal portion is simply a straight line as shown in Fig. 6. The final damage boundary shape is basically a quadrantlike infinite region, with a rounded (and possibly wiggly) corner.

It is common and usually conservative to approximate the damage boundary by its two asymptotes: v_{cr} and a_{cr}/N. These always exist, but the boundary actually dips below the horizontal asymptote for gently rising pulses and also for higher order systems where impact sets the suspension point into oscillation (if the oscillation frequency happens to approximate ω_n).

For an SDOF lightly damped linear system with a *single* damage criterion and no displacement

limit u_{cr}, and a_{cr} and v_{cr} asymptotes intersect at a point whose ray from the origin has slope ω_n or $\omega_n/2$ (the latter for fast-rising pulses). Knowing two of these three quantities (ω_n can also be determined if interior suspension dynamics are known) thus permits us to estimate the third. But if damage actually occurs in a variety of different components or for several different reasons, this intersection of asymptotes is meaningless.

Damage Boundary for General Systems

Because the damage boundary does not rely on assumptions of linearity, in principle it can be used to represent empirically the single-pulse response of any system.

For a product with multiple fragile subsystems that are reasonably linear and dynamically decoupled, the damage boundary is the outer envelope of the damage boundaries for each of the subsystems. In this case it is quite probable that the vertical asymptote comes from one subsystem and the horizontal asymptote from another. The exact shape of the region where they meet, the elbow region shown in Fig. 6, can be quite complicated and hard to determine. It is preferable to design cushioning that keeps the shock well below it.

For a product with nonlinearities or additional DOF, the horizontal region of the damage boundary can have *much more character*. Although for slowly rising pulses of extremely long duration the product shows quasistatic response, i.e., the horizontal asymptote approaches a submultiple of the permissible a_{cr}, for shorter pulses it can show extreme dips toward the Δv axis that correspond to forced resonances or acceleration amplification due to catastrophic dynamic coupling of some subunit. It is also more difficult to glean information about the interior dynamics of the product (given the multiplicity of interrelated parameters involved) from the overall damage boundary.

Determining Damage Boundary Experimentally

The damage boundary, or more typically just its asymptotes, is found by testing (ASTM, 1993; MIL-STD, 1989; Mueller, 1994). In a popular version, the product is rigidly attached to a metallic drop table (of a drop tester) that is dropped from various heights onto a gas cylinder that can be programmed to produce desired base acceleration pulses at impact. For determining the vertical asymptote of the damage boundary, shock pulse

shape does not matter. One method is to fix the gas cylinder pressure (i.e., acceleration magnitude) at a fairly high value and drop from increasing heights. (Ideally this would lead to the set of data points shown along the line of fixed a^{gas} in Fig. 7.) It must be ensured that the duration of the deceleration pulse is far less than the lowest vibration period in the product. The lowest Δv for which damage occurs is the critical velocity.

If short pulses are not practical using the gas cylinder, impact of solid metal parts (fixed spring constant) is used. In this case, collision period will be constant and peak acceleration will be proportional to drop velocity. The experimental points will fall on a line, whose slope is the shock table's natural frequency of vibration ω_{table}, or rather π/τ_{table}, where τ_{table} is impact duration as sketched in Fig. 7. As long as ω_{table} is several times *greater* than ω_n, the vertical asymptote can be found. If ω_{table} is severalfold *less* than ω_n, the horizontal asymptote can be found.

The horizontal asymptote is approached from below and is found by dropping from a fixed height onto the gas cylinder charged to increasingly high pressures. The resulting fast-rising trapezoidal pulse (used for reasons of conservatism) produces a strictly horizontal curve of ordinate a_{cr}/N. For the test to be meaningful, the collision period must be substantially longer than the vibration period and $\Delta v \geq 2v_{cr}$.

Because several drops and expendable samples are needed to establish each asymptote (ASTM, 1993; MIL-STD, 1989), it will be appreciated just how expensive it is to measure an entire damage boundary.

Usually the product is tested for impact along each of its principal axes and the damage boundary is either reported independently for each of them or as the single most fragile combination of the lowest v_{cr} and lowest a_{cr} for the entire product.

Shortcomings of SRS and Damage Boundary Approaches, and Proposals for More Thorough Fragility Testing

When using the SRS, it is important to be aware of the underlying assumptions and its limitations. The SRS is meant primarily for *linear* systems so that the base pulse response ratio can be used for cushioning design. It is also assumed in SRS analysis that failure occurs only when some critical acceleration is exceeded. For damped systems that fail when some critical displacement (or deforma-
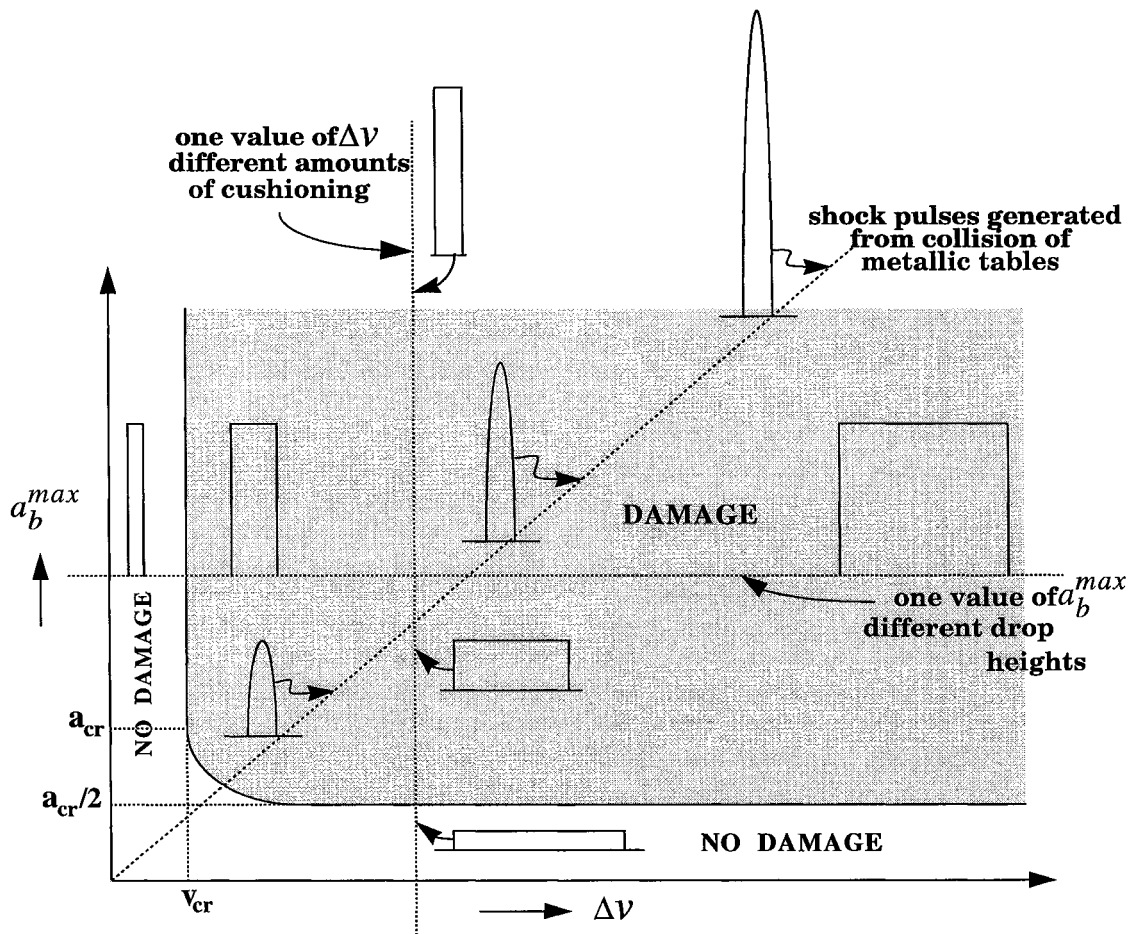
FIGURE 7 Sketch of damage boundary plot for a rectangular pulse to illustrate the shock pulses that are typically encountered during the experimental determination of the asymptotes of the damage boundary for a fragile component or product.

tion) u_{cr} is exceeded, the acceleration response is not so useful.

There are also fragile systems with finite a_{cr} and ω_n, whose acceleration has to be limited at *all* pulse lengths, i.e., $v_{cr} = 0$. One example is a disk drive with its read/write head preloaded onto the rigid platter: if the head loses contact, it will return with a high-stress impact (head slap).

An inherent limitation of an analysis of an SDOF system with a single lumped mass is that it cannot capture (without further explanations and arguments, at least) the damaging *velocity amplification* that can occur due to successive interactions between multiple masses (viz., rattling) or from the coupling between translational and rotational motions during impact of extended objects, a phenomenon we call *clattering*.

For example, in a system consisting of two unequal masses and an impact velocity of v_0, if the

heavy bottom mass rebounds elastically in a short time (compared to a light mass vibration period) suffering $\Delta v = 2v_0$, the light upper mass will eventually rebound from its upward moving base and experience $\Delta v = 4v_0$. (This principle is illustrated by the series of five unequal toy balls known as Ninja balls that are sold, for instance, by Arbor Scientific Co.) To generalize this we could say that in a purely elastic system consisting of n masses in a decreasing series, i.e., $m_i \leq m_{i-1}/3$ and $k_i \leq k_{i-1}/30$, there is a potential for the lightest, topmost mass to experience $\Delta v = 2^n v_0$. One such arrangement is illustrated in Fig. 8.

It is virtually impossible to drop a flat product (like a notebook computer or a cellular telephone) to the floor so that it lands level and bounces uniformly. Invariably one corner touches down first and there is a clattering as the various corners bounce to different heights. This is in distinct con-
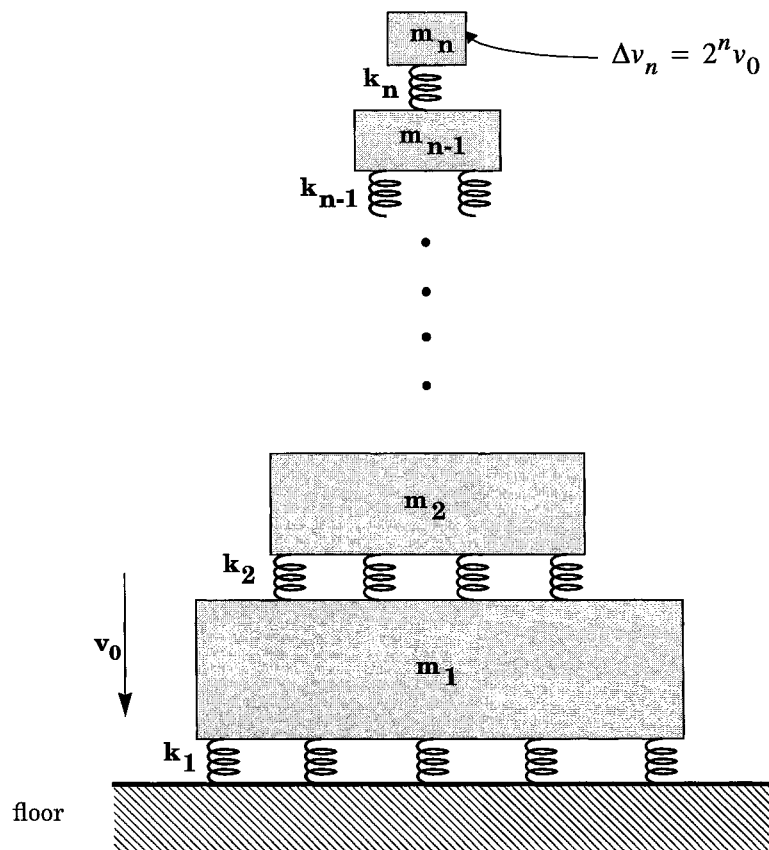
FIGURE 8 Schematic of an elastically coupled n-DOF system with their masses in the ratio $m_i \leq m_{i-1}/3$ and stiffness $k_i \leq k_{i-1}/30$ to illustrate velocity amplification.

trast to damage boundary testing, which involves a *single* impact, without rotation. For instance, in two dimensions a bar landing at a small angle from horizontal strikes at one end first and is set into rotation due to the off-centric impulsive force of contact. In the sequence of impacts that ensue, one of the ends, depending on the rod's mass distribution and coefficient of restitution, can acquire a velocity that is severalfold greater than the impact velocity and can suffer high angular accelerations as shown in Goyal et al. (1996).

Because nonlevel landing is so probable and the rotational and rapidly repeated shocks are potentially damaging, product and component fragility should be evaluated (and specified) in comparable conditions. As a preliminary recommendation, we propose that components like disk drives be mounted on hinged test carriers whose length is based on the intermediate dimension of the system for which they are destined, i.e., width rather than length or thickness. (The shorter "face" dimension gives the greater angular acceleration, because $\Delta\omega = \Delta v/L$). All tests that were formerly carried

out with products held flat to the shock table should now fix the hinge only and compliantly suspend the carrier at an angle of 10° to the table. (Perhaps all the information from this sort of testing, which includes effects of motional coupling and testing along different dimensions, could be represented in a damage boundary spanning 12-dimensional hyperspace: $\Delta v_{x,y,z}$, $\Delta\omega_{x,y,z}$, $a_{x,y,z}^{max}$, $\omega_{x,y,z}^{max}$. Speculations on the shape and attributes of such a generalized damage boundary are beyond the scope of this article.)

CUSHIONING AND SUSPENSION STRATEGIES AND GUIDELINES

In this section we consider drop protection for a system with a suspended fragile element. Assume you need to protect a disk drive within a notebook PC (as sketched in Fig. 9). How does one proceed?

Determining Fragile Component's Critical Acceleration

The first thing is to learn the drive's a_{cr}. Ideally this would be provided by the manufacturer, but it
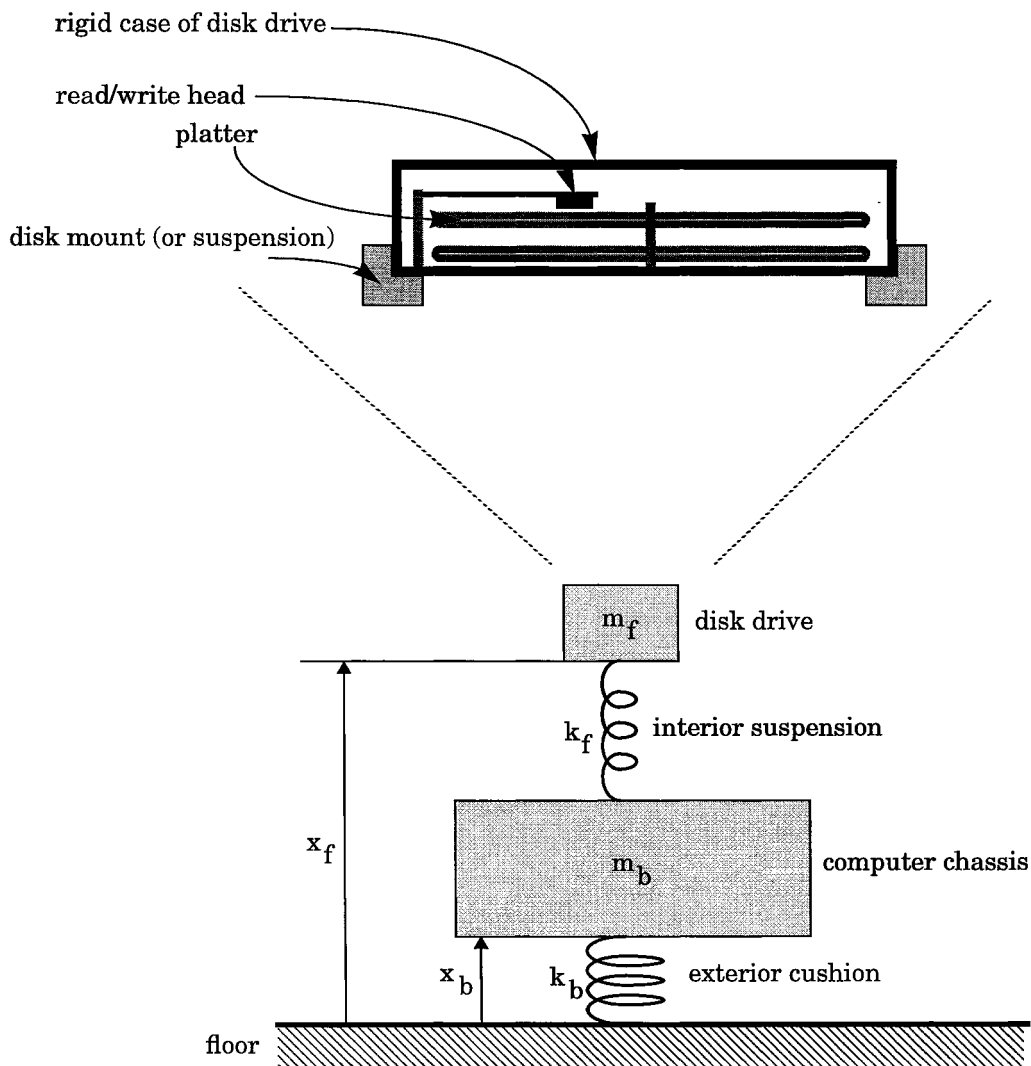
FIGURE 9 Shock analysis model for designing suspension and cushioning for a fragile device in a heavier system. Inset shows possible internal structure for the fragile device (a disk drive).

may also be determined from a slowly accelerating centrifuge test or with slowly rising pulses. (If you have to work with a complete system, the centrifuge measurement is still valid; but a drop test will provide only a_{cr}/N, unless the pulse rise time is considerably greater than the vibration period of the suspended drive.)

Normally a_{cr} should be considered an inviolable acceleration limit: the drive may not exceed it, although the chassis may, briefly. But if the drive's fragility actually arises because of a subpart (read-write head) suspended *within* it, then this internal suspension affords additional stopping distance. The drive housing may briefly exceed a_{cr}, and the drive should really be characterized by the additional quantity v_{cr}.

The essence of protection is enough *stopping distance* to limit the drive's peak acceleration. This stopping distance may be provided by exterior cushioning and/or interior suspension. As noted above, some stopping distance may even be provided by motion internal to the drive. But how much stopping distance is contributed by each compliance? Will they coordinate, so that the maximum is reached in all three simultaneously? Where does damping help?

Critical Velocity of Fragile Component

First, let us discuss the significance of the isolated drive's critical velocity. Assume the fragility is associated with an internal suspended structure of

natural frequency ω_n^{drive}. Then, as mentioned previously, the acceleration-limited critical velocity is $v_{cr}^a = a_{cr}/\omega_n^{drive}$, and a displacement-limited critical velocity is $v_{cr}^d = u_{cr}\omega_n^{drive}$. If the manufacturer wishes to maximize v_{cr} for given values of a_{cr} and u_{cr}, ω_n^{drive} should be adjusted to equal $\sqrt{a_{cr}/u_{cr}}$, in which case $v_{cr}^a = v_{cr}^d = v_{cr} = \sqrt{a_{cr}u_{cr}}$. Assuming that this has been done, or at least that the drive's critical velocity is not impact limited, then the maximum sway space available internally to the fragile element in the drive can be calculated as $u_{cr} = v_{cr}^2/a_{cr}$. (When it is impact-limited, the manufacturer should supply values not only for a_{cr} and v_{cr}, but also for either u_{cr} or ω_n^{drive}.) This calculation immediately provides a check on the test result, u_{cr} *must be* smaller than the disk drive housing, and also indicates whether the internal motion is large enough to affect cushion and suspension design.

If v_{cr} for the disk drive is greater than the Δv that is expected to be encountered in drops of the computer, perhaps no cushion or suspension is needed. Given the drop height h, and its coefficient of restitution at impact, e, Δv can be calculated by

$$\Delta v = (1 + e)\sqrt{2gh}. \tag{9}$$

If $\Delta v < v_{cr}$ no damage will occur to the drive. This is true irrespective of the surface, hard and unyielding or soft and compliant, on which the product drops. (Note that a drop onto a soft yielding surface, like a plush carpet, is likely to produce a long duration pulse, as opposed to a velocity shock. But we have shown earlier, in the section explaining the SRS plot, that the tolerable pulse area Δv^{max} for all pulse durations is $\geq v_{cr}$. Hence as long as $\Delta v < v_{cr}$, irrespective of its duration, the shock pulse is tolerable.) With no suspension and cushioning the computer can be extremely slim, with a hard case. Also the fragility of the entire PC is now characterized by the drive's a_{cr} and v_{cr}.

But note that impact restitution is important: Eq. (9) shows that when relying on short-pulse velocity absorption to protect a device, it is worthwhile to use dead, energy dissipating materials for every part and structure whose deformation affects the impact force. For a given v_{cr}, an inelastic collision with $e = 0$ *quadruples* the allowable drop height as compared to a perfectly elastic $e = 1$. Note that the coefficient of restitution is a pairwise property of the objects that impact (Goyal et al., 1994a), which in our case are the computer casing and the flooring material on which it drops. If the

floor is soft, rubbery, and elastic, the value of e could be quite high even though the casing is very dead. The designer should always keep this in mind while designing impact tolerance from a desired drop height.

In MDOF systems Δv can be many times higher than that calculated from Eq. (9) due to velocity amplification from rattling and clattering, as explained in an earlier section.

Interior Suspension Only, No Cushioning

Now let us temporarily dispense with the drive's possible internal dynamics (as indicated by its v_{cr}) and focus on chassis cushioning and drive suspension. The suspension natural frequency has already been defined as ω_n, and that of the cushioned chassis on the ground will be called Ω_n.

If $\Omega_n \gg \omega_n$, the interval during which the chassis collides with (and rebounds from) the ground is much less than the suspension vibration period. The acceleration pulse applied to the suspension point therefore qualifies as a velocity shock. In such a case, the external cushioning is quite superfluous and might as well be dispensed with (at least for the purpose of protecting the disk drive): it does not alter the velocity shock. The space it takes up is wasted. All that really matters is to make the collision *as dead as possible* to reduce the velocity shock caused by dropping from a given height.

Conversely, the interior cushioning matters a great deal. For an undamped suspension, ω_n, a_{cr}, and u_{cr} define the critical velocity for the suspended disk drive (by formulae given previously). The designer should select $\omega_n = a_{cr}/\Delta v$ and provide sway space $u_{cr} = \Delta v/\omega_n$. If the suspension can be damped to $\zeta = 0.26$ or so, an additional 20% reduction in drive acceleration will be achieved. If the suspension reacted with a more nearly constant force, the required internal sway space would approach the theoretical minimum. (One may approximate constant force by a variety of methods, beyond the addition of damping. Foamed elastomers, metallic yielding, constant-force postbuckling, and frictional slip are possible options.)

Exterior Cushion and No Suspension

On the other hand, if $\Omega_n \ll \omega_n$, the situation is effectively reversed, but comparable results may be obtained. The suspension responds quasistatically to the long acceleration pulse, and therefore is entirely superfluous. The cushioning simply must

decelerate the chassis at an acceleration no greater than a_{cr}. To effect this, select $\Omega_n = a_{cr}/v_0$; note Δv is no longer important, only the drop velocity v_0 matters. Cushion damping is not important for its effects on impact restitution (except insofar as it reduces subsequent bounces). However, cushion damping can reduce the deleterious effects of clattering as explained in Goyal et al. (1996). If the cushion approximates a constant force during deceleration, a little less stopping distance is needed. (This would again be a theoretically optimum solution.)

The only caveat is if a "perfect" constant-force material were found: its rise time would approach zero and might excite acceleration doubling oscillations in the suspension. The possibility seems remote, however.

In the two cases outlined above, near-optimal solutions were achieved by concentrating all the compliance in either the cushioning or the suspension. Outer cushioning requires more material, but it may also resist cosmetic scuffing better and reduce sensitivity to compliance of the floor. It protects every internal fragile system and need not necessarily be damped. Inner suspension uses less energy-absorbing material and offers environmental isolation (the material need not resist UV degradation nor need it be safe for babies to chew on). On the other hand, while the base acceleration pulse is often unimodal, the suspension motion is likely to be oscillatory (unless intentionally damped), and these oscilaltions can potentially excite resonance of interior drive structures. Additionally the rigid casing has to be energy dissipating which, given its low compliance, is not an easy task. On the whole it would seem that in most cases concentrating all the compliance in the cushioning is somewhat preferable over having it all in the suspension!

Why Combination of Cushioning and Suspension Is Not Optimal

An arrangement in which both cushioning and suspension are present cannot improve on the above approaches, but it can certainly do worse. Qualitatively speaking, the natural frequencies Ω_n and ω_n cannot be very different, or the higher one will contribute nothing to the stopping distance. On the other hand, if they are too similar, the risk arises of damaging interactions.

We can make this assertion precise for the specific case of an elastic (half-sine) base acceleration and undamped suspension. We do this by using

the SRS to calculate the amplification of a base pulse, then scaling cushion and/or suspension stiffnesses so that the peak fragile-mass acceleration equals a_{cr}. Finally, the peak cushion and suspension displacements are added and plotted as a function of stiffness ratio.

Assume that the masses of base and fragile element are given, and that the ratio of suspension stiffness k_f to cushion stiffness k_b is to be explored. Then $\omega_n/\pi\Omega_n$ forms a convenient independent variable, in particular because for half-sine pulses,

$$\frac{T_{eff}}{T_n} = \frac{\omega_n}{\pi\Omega_n}, \tag{10}$$

so that the SRS response function can be written as $R(\omega_n/\pi\Omega_n)$, or more briefly as $R(\alpha)$. For a given drop velocity v_0, the base acceleration pulse magnitude $a_b^{max} = v_0\Omega_n$ and the corresponding peak fragile-mass acceleration is

$$a_f^{max} = v_0\Omega_n R(\alpha). \tag{11}$$

Setting this acceleration to equal a_{cr} yields

$$\Omega_n = \frac{a_{cr}}{v_0 R(\alpha)}. \tag{12}$$

The magnitude of cushion displacement x_b^{max} and suspension deformation u_{max} are

$$x_b^{max} = \frac{v_0}{\Omega_n} = \frac{v_0^2}{a_{cr}} R(\alpha),$$

$$u^{max} = \frac{a_{cr}}{\omega_n^2} = \frac{a_{cr}}{\pi^2\Omega_n^2\alpha^2} = \frac{v_0^2}{a_{cr}}\left(\frac{R(\alpha)}{\pi\alpha}\right)^2. \tag{13}$$
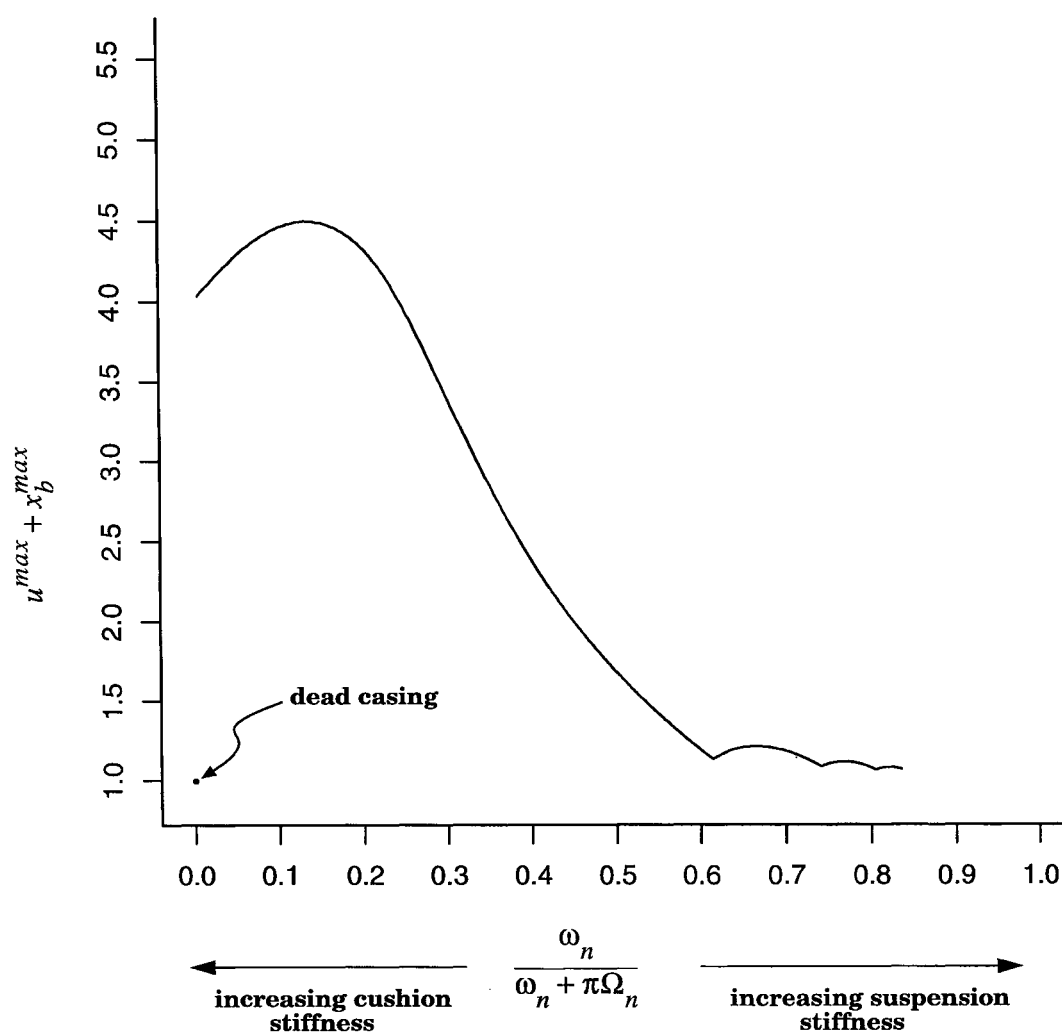
Adding the two to get total displacement yields

$$u^{max} + x_b^{max} = \frac{v_0^2}{a_{cr}}\left(\left(\frac{R(\alpha)}{\pi\alpha}\right)^2 + R(\alpha)\right). \tag{14}$$

The above expression for total displacement is independent of individual stiffnesses or masses, depending only on the natural frequency ratio α. To plot it conveniently, we remap α onto the interval $[0, 1)$ via the transformation $\alpha/(\alpha + 1)$. Note that

$$\frac{\alpha}{\alpha + 1} = 0 \Rightarrow \Omega_n \to \infty \Rightarrow k_b \to \infty,$$

$$\frac{\alpha}{\alpha + 1} \to 1 \Rightarrow \omega_n \to \infty \Rightarrow k_f \to \infty.$$

FIGURE 10 Plot of total displacement (normalized) of fragile device $u^{max} + x_b^{max}$ as a function of suspension and cushion stiffness ratio $\omega_n/(\omega_n + \pi\Omega_n)$ for the system of Fig. 9.

The resulting plot of total displacement (normalized by v_0^2/a_{cr}) versus $\alpha/(\alpha + 1)$, plotted in Fig. 10, shows that either extreme of natural frequency ratio uses less total cushioning plus suspension distance than in the middle, although the advantage at the $\alpha = 0$ end (velocity shock region) appears unimpressive. But note that in the above analysis it has been implicitly assumed that the collision is completely elastic so that Δv imparted to the base is $2v_0$. Recall, however, that in the velocity shock regime we recommend that for real products the stiff housing be dead, i.e., $\Delta v = v_0$. This implies that the required suspension deformation $u^{max} = (\Delta v)^2/a_{cr} = v_0^2/a_{cr}$, which is *one-fourth* the value shown in the plot and matches the minimum at the $\alpha = 1$ end! The conclusion is that there is nothing to recommend the combination of cushioning with suspension.

In light of the above conclusion, let us return to the case of a disk drive with internal dynamics and a critical velocity v_{cr}. Assuming this critical velocity is acceleration limited (i.e., not due to internal collisions), then it reflects the existence of a minimum internal stopping distance of v_{cr}^2/a_{cr}. The greater the critical velocity of the disk drive, the more the desire of the designer to exploit the internal stopping distance it implies. But in fact it is not possible to use it: that internal sway space is wasted, and in fact a greater v_{cr} may increase the potential for damage!

The argument is simply a repeat of the above, where we concluded that all compliance should be concentrated, either in the cushioning or in the suspension. Recall that for a given a_{cr}, greater v_{cr} is achieved by increasing available internal sway space and reducing ω_n^{drive} to a_{cr}/v_{cr}. But a very low

ω_n^{drive} means that the cushioning provides a velocity shock, so its brief compression is wasted. If the internal natural frequency approximates the cushion or suspension natural frequency, dynamic amplification will exacerbate damage. (This is particularly a concern if the interior suspension has an oscillatory response, which drives the internal suspension into resonance.) And finally a high ω_n^{drive} (and low v_{cr}) means that the internal suspension does not deform and, therefore, does not contribute meaningfully to the total fragile-element stopping distance. (The internal space is wasted.)

Therefore, unless disk drive v_{cr} is sufficiently great to protect against anticipated drops, it is *far better* to make it *as small as possible.*

SUMMATION AND DISCUSSION

The problem of improving the impact tolerance of portable electronic products, for a broader set of market segments, presents several design challenges due to the extreme nature (short duration and high magnitude) of impact forces and stringent constraints on acceptable weight and size of these objects. Analytically this is a tough problem because the complicated interactions that occur between (and within) the components of the product during impact are hard to model in their entirety.

By focusing on some subsidiary fragile subpart of the product and modeling it as a SDOF linear system whose motion does not affect that of the heavier casing, the SRS analysis plots the fragile-part peak acceleration in response to unimodal shock pulses of various shapes and durations applied to its base. It is additionally assumed that the fragile part is damaged if some critical acceleration a_{cr} is exceeded. The important message that emerges from SRS analysis is that shock pulse duration is critical to determining fragile-part peak acceleration: if this duration is small compared to fragile-part response time, it is experienced as a velocity shock and peak acceleration depends only on the velocity that the shock pulse imparts and not its magnitude; if the duration is fairly long compared to response time, peak acceleration will depend only on shock pulse magnitude and rise time. Fast rise times elicit high transient responses. The concept of velocity shock leads to the notion of critical velocity v_{cr}, i.e., a shock pulse velocity threshold below which the part is not damaged. The long-duration pulse response clarifies the main purpose of cushioning, which is to increase the duration of the shock pulse and reduce its magnitude. We argue that the above asymptotic

fragile-part response behaviors are true for more general systems than included in the SRS analysis.

Another plot that separates safe shock pulses from damage causing ones based on their area and magnitude is the damage boundary. The asymptotes of the damage boundary (a semiinfinite, quadrantlike region) are related to v_{cr} and a_{cr} and are found by testing, although this may be expensive and tedious. Although the damage boundary is applicable to more general systems than the SRS, it is correspondingly harder to interpret for improving system shock tolerance.

We point out some nonobvious limitations of the SRS and damage boundary approaches, viz., their inability to directly illustrate the damaging velocity amplification that can occur in multiple mass systems and extended objects due to rattling and clattering. We propose a slight modification to the damge boundary testing procedure that can ddress the issue of rotational impacts to some extent. The SRS and damage boundary form the theoretical basis underlying industry standard shock evaluation tests (ASTM D3332 and MIL-STD-810); hence, it is important that the assumptions and limitations be understood for correctly performing these tests and accurately interpreting their results.

Finally we discussed some general packaging and shock-mounting strategies in the context of protecting a fragile disk drive in a notebook computer. For the slenderest form factor, we argue that cushioning should all be concentrated on the outside of the unit and be moderately damped. As a second choice, all the space may be utilized inside for suspending the disk drive, and the hard outer shell should be dead, i.e., have inelastic collisions with the ground. Using both cushioning and suspension is inadvisable: it wastes space and could even increase the potential for damage. The stiffnesses (or natural frequencies) of internal suspension must be adjusted so that components and fragile elements do not bang into each other during impact; i.e., they should have ample sway space. Unless the drive's critical velocity is greater than the drop velocity, we have shown, somewhat counter to intuition, that it is best to make the disk drive as thin as possible and thus keep its critical velocity small.

APPENDIXES

Peak Acceleration of Spring-Mass Damper System

In this section we derive the expressions for peak acceleration of a spring-mass damper system (like

the one composed of the fragile mass and its suspension in Fig. 1), subject to various initial conditions. The equation of motion for the system is given as

$$m\ddot{x} + c\dot{x} + kx = 0. \tag{A.1}$$

Initial Velocity Condition

$$x(0) = 0, \quad \dot{x}(0) = v_0.$$

This corresponds to the system being subjected to a velocity shock of magnitude v_0.

The solution to Eq. A.1 is then given as

$$x(t) = \frac{v_0}{\omega_d} e^{-\zeta\omega_n t} \sin(\omega_d t), \tag{A.2}$$

where $\omega_d = \omega_n\sqrt{1-\zeta^2}$. Acceleration for the system is

$$\ddot{x}(t) = \frac{v_0\omega_n e^{-\zeta\omega_n t}}{\sqrt{1-\zeta^2}}((2\zeta^2 - 1)\sin(\omega_d t) \\ - 2\zeta\sqrt{1-\zeta^2}\cos(\omega_d t)). \tag{A.3}$$

To find the time, t^*, at which peak accleration occurs, we differentiate Eq. (A.3) and set the result to zero, yielding

$$\frac{v_0\omega_n^2 e^{-\zeta\omega_n t}}{\sqrt{1-\zeta^2}}(\sqrt{1-\zeta^2}(4\zeta^2 - 1)\cos(\omega_d t)$$

$$+ \zeta(3 - 4\zeta^2)\sin(\omega_d t)) = 0.$$

$$\Rightarrow \tan(\omega_d t^*) = \frac{\sqrt{1-\zeta^2}(4\zeta^2 - 1)}{\zeta(4\zeta^2 - 3)},$$

$$\sin(\omega_d t^*) = -\sqrt{1-\zeta^2}(4\zeta^2 - 1),$$

$$\cos(\omega_d t^*) = -\zeta(4\zeta^2 - 3).$$

Substituting the above in Eq. A.3 gives the peak acceleration as

$$\ddot{x}^{\max} =$$

$$\begin{cases} -\dfrac{\zeta}{\sqrt{1-\zeta^2}}\tan^{-1}\left(\dfrac{\sqrt{1-\zeta^2}(4\zeta^2-1)}{\zeta(4\zeta^2-3)}\right) \\ -v_0\omega_n e & \text{for } 0 \le \zeta \le 0.5, \\ -2v_0\omega_n\zeta & \text{for } 0.5 < \zeta \le 1, \end{cases} \tag{A.4}$$

Note that for $\zeta > 0.5$, the initial acceleration is the peak acceleration; i.e., $\ddot{x}(0) = \ddot{x}^{\max} = -2v_0\omega_n\zeta$.

Also, $\ddot{x}^{\max}$ can be made arbitrarily large by increasing ζ.

Initial Displacement Condition

$$x(0) = x_0, \quad \dot{x}(0) = 0.$$

This initial condition can be used to calculate the response of the system to a step change in acceleration of magnitude $a_b^{\max}$ applied to its base (like with a long-duration rectangular pulse). Within the accelerated system thus created, the fragile mass will oscillate about a mean equilibrium position with relative displacement amplitude $x_0 = ma_b^{\max}/k = a_b^{\max}/\omega_n^2$.

Solving Eq. (A.1), subject to the above initial conditions, gives

$$x(t) = x_0 e^{-\zeta\omega_n t}\left(\cos(\omega_d t) + \frac{\zeta}{\sqrt{1-\zeta^2}}\sin(\omega_d t)\right), \tag{A.5}$$

$$\ddot{x}(t) = \frac{x_0\omega_n^2 e^{-\zeta\omega_n t}}{\sqrt{1-\zeta^2}}\left(\zeta\sin(\omega_d t) - \sqrt{1-\zeta^2}\cos(\omega_d t)\right). \tag{A.6}$$

Again, the search for t^* yields

$$\frac{x_0\omega_n^3 e^{-\zeta\omega_n t}}{\sqrt{1-\zeta^2}}(2\zeta\sqrt{1-\zeta^2}\cos(\omega_d t)$$

$$+ (1 - 2\zeta^2)\sin(\omega_d t)) = 0$$

$$\Rightarrow \tan(\omega_d t^*) = \frac{2\zeta\sqrt{1-\zeta^2}}{2\zeta^2 - 1},$$

$$\sin(\omega_d t^*) = 2\zeta\sqrt{1-\zeta^2},$$

$$\cos(\omega_d t^*) = 2\zeta^2 - 1.$$

Substituting the above in Eq. (A.6) gives the peak acceleration to be

$$\ddot{x}^{\max} = \begin{cases} x_0\omega_n^2 e^{-\frac{\zeta}{\sqrt{1-\zeta^2}}\left(\tan^{-1}\left(\frac{2\zeta\sqrt{1-\zeta^2}}{2\zeta^2-1}\right)+\pi\right)} \\ \qquad\qquad\qquad \text{for } 0 \le \zeta \le \sqrt{0.5}, \\ x_0\omega_n^2 e^{-\frac{\zeta}{\sqrt{1-\zeta^2}}\tan^{-1}\left(\frac{2\zeta\sqrt{1-\zeta^2}}{2\zeta^2-1}\right)} \\ \qquad\qquad\qquad \text{for } \sqrt{0.5} < \zeta \le 1. \end{cases} \tag{A.7}$$

Equation (A.7) shows that $\ddot{x}^{\max}$ has a maximum value of $x_0\omega_n^2$ for $\zeta = 0$.

Acceleration of Fragile Mass for Various Pulse Shapes

In this section we present the acceleration response of a linear spring-mass system (zero damping) when subjected to basal excitation pulses of various shapes. These results are adapted from Ayre (1988). They were used to generate the response ratios plotted in the SRS curves of Figs. 3 and 4 and the damage boundary plots in Fig. 6.

Rectangular Pulse. A rectangular excitation pulse of actual duration τ can be written as

$$a_b(t) = \begin{cases} a_b^{max} & \text{for } 0 \le t \le \tau, \\ 0 & \text{for } t \ge \tau. \end{cases} \tag{A.8}$$

The corresponding fragile-mass acceleration is then given as

$$\ddot{x}_f(t) = \begin{cases} a_b^{max}(1 - \cos(\omega_n t)) & \text{for } 0 \le t \le \tau, \\ 2a_b^{max}\sin\left(\dfrac{\pi\tau}{T_n}\right)\sin\left(\omega_n(t - \dfrac{\tau}{2})\right) & \text{for } t \ge \tau. \end{cases} \tag{A.9}$$

Half-Sine Pulse. The pulse, as a function of its actual duration τ, may be written as

$$a_b(t) = \begin{cases} a_b^{max} \sin\left(\dfrac{\pi t}{\tau}\right) & \text{for } 0 \le t \le \tau, \\ 0 & \text{for } t \ge \tau, \end{cases} \tag{A.10}$$

and the corresponding fragile-mass acceleration is

$$\ddot{x}_f(t) =$$
$$\begin{cases} a_b^{max}\dfrac{4\tau^2}{4\tau^2 - T_n^2}\left(\sin\left(\dfrac{\pi t}{\tau}\right) - \dfrac{T_n}{2\tau}\sin(\omega_n t)\right) & \text{for } 0 \le t \le \tau, \\ a_b^{max}\dfrac{4\tau T_n}{T_n^2 - 4\tau^2}\cos\left(\dfrac{\pi\tau}{T_n}\right)\sin\left(\omega_n\left(t - \dfrac{\tau}{2}\right)\right) & \text{for } t \ge \tau. \end{cases} \tag{A.11}$$

Versed Sine Pulse. The pulse, as a function of its actual duration τ, may be written as

$$a_b(t) = \begin{cases} \dfrac{a_b^{max}}{2}\left(1 - \cos\left(\dfrac{2\pi t}{\tau}\right)\right) & \text{for } 0 \le t \le \tau, \\ 0 & \text{for } t \ge \tau, \end{cases} \tag{A.12}$$

and the corresponding fragile-mass acceleration is

$$\ddot{x}_f(t) =$$
$$\begin{cases} a_b^{max}\dfrac{T_n^2}{2T_n^2 - 2\tau^2}\left(1 - \dfrac{\tau^2}{T_n^2} + \dfrac{\tau^2}{T_n^2}\cos\left(\dfrac{2\pi t}{\tau}\right) - \cos(\omega_n t)\right) & \\ & \text{for } 0 \le t \le \tau, \\ a_b^{max}\dfrac{T_n^2}{T_n^2 - \tau^2}\sin\left(\dfrac{\pi\tau}{T_n}\right)\sin\left(\omega_n\left(t - \dfrac{\tau}{2}\right)\right) & \\ & \text{for } t \ge \tau. \end{cases} \tag{A.13}$$

Symmetrical-Triangular Pulse. The pulse, as a function of its actual duration τ, may be written as

$$a_b(t) = \begin{cases} 2a_b^{max}\dfrac{t}{\tau} & \text{for } 0 \le t \le \dfrac{\tau}{2}, \\ 2a_b^{max}\left(1 - \dfrac{t}{\tau}\right) & \text{for } \dfrac{\tau}{2} \le t \le \tau, \\ 0 & \text{for } t \ge \tau, \end{cases} \tag{A.14}$$

and the corresponding fragile-mass acceleration is

$$\ddot{x}_f(t) =$$
$$\begin{cases} 2a_b^{max}\left(\dfrac{t}{\tau} - \dfrac{T_n}{2\pi\tau}\sin(\omega_n t)\right) & \\ & \text{for } 0 \le t \le \dfrac{\tau}{2}, \\ 2a_b^{max}\left(1 - \dfrac{t}{\tau} - \dfrac{T_n}{2\pi\tau}\sin(\omega_n t) + \dfrac{T_n}{\pi\tau}\sin\left(\omega_n\left(t - \dfrac{\tau}{2}\right)\right)\right) & \\ & \text{for } \dfrac{\tau}{2} \le t \le \tau, \\ a_b^{max}\dfrac{4T_n}{\pi\tau}\sin^2\left(\dfrac{\pi\tau}{2T_n}\right)\sin\left(\omega_n\left(t - \dfrac{\tau}{2}\right)\right) & \\ & \text{for } t \ge \tau. \end{cases} \tag{A.15}$$
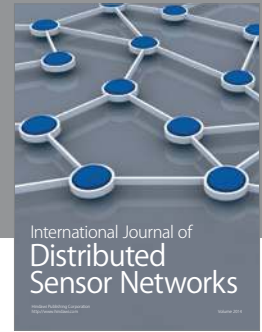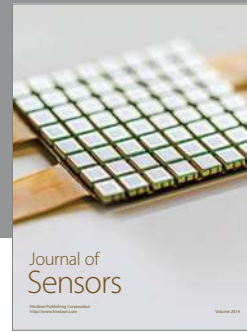
ACKNOWLEDGMENTS

REFERENCES

ASTM D 3332-88, "Standard Test Methods for Mechanical-Shock Fragility of Products, Using Shock Machines," in *1993 Annual Book of ASTM Standards,* 1993, Vol. 15.09, Philadelphia, PA.

Ayre, R. S., "Transient Response to Step & Pulse Functions," in *Shock & Vibration Handbook*, 1988, McGraw-Hill Book Company, New York, Chap. 8.

Goyal, S., Papadopoulos, J. M., and Sullivan, P. A., 1996, "The Dynamics of Clattering: Multiple Impacts of Tilted Objects," Technical Memorandum, Bell Laboratories, Murray Hill, NJ.

Goyal, S., Pinson, E. N., and Sinden, F. W., 1994a, "Simulation of Dynamics of Interacting Rigid Bodies Including Friction I: General Problem and Contact Model," *Engineering with Computers*, Vol. 10, Springer–Verlag, London, pp. 161–173.

Goyal, S., Pinson, E. N., and Sinden, F. W., 1994b, "Simulation of Dynamics of Interacting Rigid Bodies Including Friction II: Software System Design and Implementation," *Engineering with Computers*, Vol. 10, Springer–Verlag, London, pp. 175-195.

Henderson, G., 1993, "SRS Analysis for Protective Package Engineering & Testing," Technical Bulletin, GHI Systems, Inc., San Pedro, CA.

MIL-STD-810E, 1989, *Military Standard Environmental Test Methods and Engineering Guidelines*, U.S. Office of Naval Publications, Washington, DC.

Mindlin, R. D., 1945, "Dynamics of Package Cushioning," *Bell Systems Journal*, Vol. 24, pp. 353–461.

Mueller, C., and Lee, M., 1994, "Maxtor's Damage Boundary Test Methods," Technical Product Bulletin, Maxtor Corporation, San Jose, CA.

Newton, R. E., 1968, "Fragility Assessment Theory and Test Procedure," Technical Report, U.S. Naval Postgraduate School, Monterey, CA.

Newton, R. E., "Theory of Shock Isolation," in *Shock & Vibration Handbook*, 1988, McGraw–Hill Book Company, New York, Chap. 31.

Newton, R. E., 1989, "The Damage Boundary Revisited," Report 89-WA/EEP-24, ASME, New York.

Rubin S., "Concepts in Shock Data Analysis," in *Shock & Vibration Handbook*, 1988, McGraw–Hill Book Company, New York, Chap. 23.